

Synthesis and Size-Controllable Self-Assembly of a Novel Amphiphilic Hyperbranched Multiarm Copolyether

Yiyong Mai, Yongfeng Zhou,* and Deyue Yan*

College of Chemistry and Chemical Engineering, Shanghai Jiao Tong University,
800 Dongchuan Road, Shanghai 200240, P. R. China

Received June 27, 2005; Revised Manuscript Received August 10, 2005

ABSTRACT: A series of novel hyperbranched multiarm copolyethers of PEHO-*star*-PPO with different molar ratios of PPO arms to PEHO cores ($R_{A/C}$) were synthesized. NMR and SEC measurements confirm the molecular structure of PEHO-*star*-PPOs. Both glass transition temperature (T_g) and decomposition temperature (T_d) of PEHO-*star*-PPO decrease with increasing $R_{A/C}$. The self-assembly behavior of PEHO-*star*-PPO copolymers was investigated by TEM, SEM, DLS, etc. The results indicate that the ill-defined PEHO-*star*-PPO molecules could aggregate into large spherical micelles (over 100 nm) with controlled sizes, and the micelle size decreases as $R_{A/C}$ increases. The structure of the large micelles was explored by FT-IR, NMR, etc. Accordingly, a possible self-assembly process is put forward, and a new aggregate model termed as multimicelle aggregate (MMA) (Figure 9C) is suggested to explain the formation of the large micelles. In MMA model, the large micelles are the aggregates of small micelles associated by intermicellar interactions such as hydrogen bonds.

Introduction

In recent decades, molecular self-assembly has always been an active topic of research because it produces a variety of nanoobjects with various beautiful shapes,¹ which have potential technological applications in many research fields such as medicine, biochemistry, and material science.² For example, micelles, the most prevalent objects of self-assembly, can be widely used in drug delivery systems³ and used as the template for the preparation of nano- or mesoscale materials.⁴

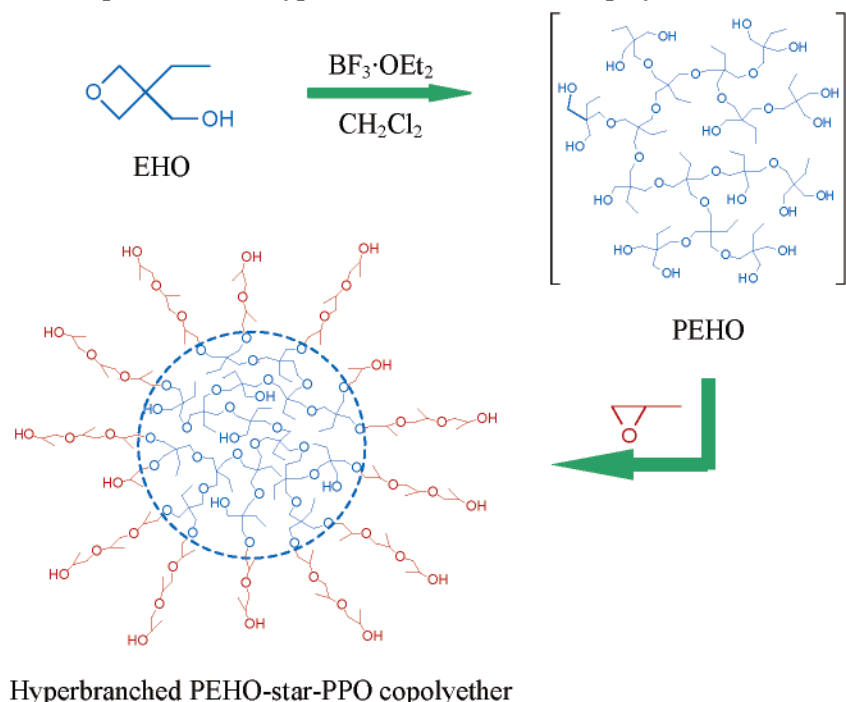
In the pioneer works reported by Eisenberg and co-workers,⁵ multiple morphologies of “crew-cut” micelles made from amphiphilic linear block copolymers, such as large compound micelles (LCMs), vesicles, rods, etc., have been observed. Furthermore, they found some major factors that influence the morphology and dimension of the self-assembly aggregates, including the composition of the copolymer, the concentration of the polymer solution, the ambient temperature, the solvent, and so on. Likewise, many other scientists have designed and prepared various new amphiphilic molecules with special architectures in order to obtain novel self-assembled objects with particular morphologies.⁶ However, most researchers mainly focused on the molecular self-assembly of well-defined molecules, including linear block copolymers,⁵ small amphiphiles,⁷ and dendrimers.⁸ Little attention has been paid to the self-assembly originating from ill-defined macromolecules such as hyperbranched copolymers. Recently, this laboratory prepared a novel amphiphilic hyperbranched multiarm copolyether with a hydrophobic hyperbranched poly[3-ethyl-3-(hydroxymethyl)oxetane] core (PEHO)⁹ and many hydrophilic poly(ethylene glycol) arms (PEO).¹⁰ The obtained copolymer of PEHO-*star*-PEO^{10c} possesses several special characteristics in structure. First, it is an ill-defined copolymer based on a hyperbranched core. Second, both the core and arms of the copolymer consist

of flexible polyethers, which is favorable for the conformation transition of the copolymer during the self-assembly process. Third, there is a big difference of hydrophilicity between PEO arms and PEHO cores, which is capable of driving the phase separation of the amphiphilic hyperbranched molecules in some selective solvents. Interestingly, the authors have found that the ill-defined PEHO-*star*-PEO copolymers can directly self-assemble into macroscopic tubes in acetone^{10a} and giant polymer vesicles in water.^{10b}

In this work, we present a new hyperbranched multiarm copolyether, PEHO-*star*-PPO, which is prepared by the one-pot, two-step cationic ring-opening polymerization of 3-ethyl-3-(hydroxymethyl)oxetane and propylene oxide¹¹ (Scheme 1). PEHO-*star*-PPO is similar to PEHO-*star*-PEO, for instance, the ill-defined architecture and the flexibility of polyethers. However, the difference in the hydrophilicity between PPO arms and PEHO cores in PEHO-*star*-PPO is much smaller than that in PEHO-*star*-PEO. It led to a question of whether the ill-defined copolymers with such a poorer amphiphilic property as PEHO-*star*-PPO could self-assemble or not.

Interestingly, the answer is positive. We found that PEHO-*star*-PPO can self-assemble into large spherical micelles (> 120 nm) with controlled sizes, and the size is dependent on the molar ratios of PPO arms to PEHO cores ($R_{A/C}$: “A” in the subscript means arms and “C” means cores). To our knowledge, most conventional micelles are in the size scale smaller than 100 nm.¹² The micelle with a diameter larger than 100 nm is special and no longer amenable to the self-assembly mechanism based on conventional small micelles. So a new mechanism should be provided to demonstrate the formation of large micelles. The “LCM” model presented by Eisenberg et al.^{5a,b} successfully explained the large micelles (up to 1200 nm) formed by PS-*b*-PAA linear copolymers. Müller and Abetz et al.¹³ logically explained the formation of “supermicelles” (over 100 nm) by the further aggregation of “Janus micelles” formed by PS-*b*-PB-*b*-PMAA triblock copolymers. However, because of

* To whom correspondence should be addressed: Tel +86-21-54742665; Fax +86-21-54741297; e-mail yfzhou@sjtu.edu.cn or dyyan@sjtu.edu.cn.

Scheme 1. Preparation of a Hyperbranched Multiarm Copolyether of PEHO-*star*-PPO

the difference in architecture between linear block copolymers and hyperbranched multiarm copolymers, it seems necessary to find a different mechanism for the self-assembly of ill-defined PEHO-*star*-PPO molecules. In this work, a possible mechanism based on multimicelle aggregate (MMA) is suggested to elucidate the formation of large micelles.

Experimental Section

Preparation of PEHO-*star*-PPOs. In a dried three-necked round-bottomed flask with a funnel and a thermometer, 3-ethyl-3-(hydroxymethyl)oxetane (EHO) was added into the solution of $\text{BF}_3 \cdot \text{OEt}_2$ in dried CH_2Cl_2 under an argon atmosphere (the molar ratio of EHO to $\text{BF}_3 \cdot \text{OEt}_2$ is 2:1). The reaction mixture was stirred vigorously at 0 °C for 48 h to form PEHO precursor. A part of the precursor was withdrawn by syringe for characterization. In succession, the calculated amount of propylene oxide (PO) was dropwise added into the precursor solution (kept the temperature of the reaction mixture around −20 °C). After the addition of PO, the reaction was kept for another 24 h under stirring condition at −20 °C. A small amount of pure water was then added into the reaction system to quench the cationic copolymerization. The resulting solution was washed by cold deionized water for at least three times to remove PPO homopolymer and other organic small molecules. After water was eliminated completely, the CH_2Cl_2 solvent was removed under reduced pressure at 30 °C. A viscous jelly like product was then acquired. If the added amount of PO was varied, PEHO-*star*-PPO samples with different $R_{\text{A/C}}$ and high yields (>50%) were obtained (Table 1,

P1–P5). The synthesis process and structure of the copolymers are shown in Scheme 1.

Micellization of PEHO-*star*-PPOs. At ambient temperature around 15 °C, 10 mg of PEHO-*star*-PPO sample was dissolved in 5 mL of DMSO before use. Under the gentle stirring, deionized water was added dropwise into the solution until the weak blue light appeared. Then, an excess of water was added into the solution to stabilize the self-assembly morphology. After quenching, the solution was dialyzed against deionized water to remove DMSO solvent, leaving a very dilute aqueous solution of the aggregates. The final concentration of each PEHO-*star*-PPO sample in the resultant solution was set to 0.2 g/L.

Measurements. NMR Measurements. ^1H NMR and ^{13}C NMR measurements were performed on a Varian MERCURYplus 400 spectrometer in $\text{DMSO}-d_6$ at 20 °C. TMS was used as the internal reference.

Size Exclusion Chromatography (SEC). The molecular weights of the products were measured by SEC on a Perkin-Elmer Series 200 system at 70 °C (100 μL injection column, PL gel (10 μm) 300 mm \times 7.5 mm mixed-B columns, polystyrene calibration). DMF was used as the solvent, and the flow rate was 1.0 mL/min.

Differential Scanning Calorimetry (DSC). Glass transition temperatures (T_g) of the products were measured on a TA MDSC2910 apparatus at a heating rate of 10 °C/min from −100 to 150 °C.

Thermal gravimetric analysis (TGA) was carried out on a Perkin-Elmer TGA-7 instrument with a heating rate of 20 °C/min in the nitrogen flow (20 mL/min).

Table 1. Characterizations of PEHO-*star*-PPO Samples

sample	R_{feed}^a	$R_{\text{A/C}}^b$	SEC		$M_{\text{n,NMR}}^c$	T_g^d (°C)	T_d^e (°C)
			$M_{\text{n,core}}$ (PDI)	$M_{\text{n,sample}}$ (PDI)			
P1	1:1	0.8	7300 (1.75)	9890 (1.72)	10220	−21.4	358
P2	2:1	1.6	7370 (1.71)	12400 (1.60)	13270	−39.7	317
P3	5:1	4.0	6380 (1.66)	16050 (1.43)	19140	−59.5	265
P4	10:1	6.8	6430 (1.68)	20750 (1.39)	28290	−66.1	243
P5	20:1	9.2	6250 (1.63)	26130 (1.30)	35000	−66.7	218

^a R_{feed} is the feed ratio of PO to EHO monomer. ^b $R_{\text{A/C}}$, the molar ratio of PPO arms to PEHO cores, is determined by ^1H NMR. ^c $M_{\text{n,NMR}} = M_{\text{n,core}} + R_{\text{A/C}} \times M_{\text{n,core}} \times \text{MW}_{\text{PPO}}/\text{MW}_{\text{PEHO}}$. ^d PEHO has a T_g of about 40 °C²² and linear PPO has a T_g of around −75 °C.^{18a} ^e Herein T_d was the temperature at which copolymers lost their 5% of weights; PEHO core has a T_d of ~365 °C.

Variable temperature FT-IR was conducted on a Perkin-Elmer Paragon 1000 instrument from 20 to 170 °C. The micellar solutions were coated on silicon wafers, and the samples were carefully dried before measurement.

Dynamic light scattering (DLS) measurements were performed in aqueous solution using a Malvern Zetasizer 3000 HS apparatus (Malvern Instruments Ltd.) equipped with a 125 mW laser operating at $\lambda = 633$ nm. All the DLS were measured at 15 ± 0.1 °C and at a scattering angle of 90°. The CONTIN program, developed by Provencher,¹⁴ was used in the Laplace inversion of the correlation function to obtain $G(\Gamma)$, and $G(\Gamma)$ can be converted into a transitional diffusion coefficient distribution $G(D)$ or a hydrodynamic diameter distribution $f(D_h)$ via the Stokes–Einstein equation,¹⁵ $D_h = k_B T / 3\pi\eta D$, where k_B , T , and η are the Boltzmann constant, the absolute temperature, and the solvent viscosity, respectively.

Transmission electron microscopy (TEM) studies were performed with a JEOL JEM-100CX-II instrument at a voltage of 100 kV. Samples were prepared by drop-casting micellar solutions onto carbon-coated copper grids and were air-dried at room temperature before measurement.

Scanning electron microscopy (SEM) observations were conducted on a Philips Sirion 200 at an accelerating voltage of 10 kV. The specimens for SEM observations were prepared by depositing several drops of micellar solutions onto silicon wafers and were dried in a vacuum at room temperature.

Results and Discussion

Preparation and Characterizations of PEHO-star-PPOs. Synthesis of multiarm star copolymers with amphiphilic segments has attracted much attention at present because of their potential applications.¹⁶ Both “arm-first”¹⁷ and “core-first”¹⁸ methods have been developed to get multiarm copolymers. In this work, the “core-first” method was adopted to prepare PEHO-star-PPO samples (Scheme 1). The resulting products (P1–P5 in Table 1) were colorless viscous liquids, and their apparent viscosities became smaller with increasing the length of PPO arms. Interestingly, PEHO powders precipitated immediately when PEHO solution in CH_2Cl_2 was poured into water; however, the precipitation did not occur to PEHO-star-PPO solutions in a similar procedure. The copolymers still dissolved in the organic phase below water layer. Evidently, water is no longer a good precipitate agent for PEHO-star-PPOs. It shows that PPO arms have been covalently linked to PEHO cores, giving rise to the better hydrophilicity of the copolymers. Furthermore, the phenomena indicate that the hydrophilicity of PPO is better than that of PEHO. It is well-known that PPO is poorer than PEO in hydrophilicity. So the self-assembly behavior of PEHO-star-PPO samples would be different from that of PEHO-star-PEO molecules reported previously.^{10b}

The structure of the prepared copolymers is confirmed by ^1H NMR and ^{13}C NMR. The ^1H NMR spectra and assignments are given in Figure 1. Identical with our predictions, the intensity of PPO signals (**f**, **g**, **h**, **i**, and **j**)^{18a} amplifies gradually with increasing the feed ratio (R_{feed}) of PO to EHO and the $-\text{OH}$ peak of PEHO core (**e**) decreases and finally disappears as the R_{feed} increases. The result indicates that the units of PO have been covalently linked to PEHO cores. On the other hand, to express the amount of PO units grafted to PEHO cores, the molar ratio of PPO arms to PEHO cores ($R_{\text{A/C}}$) was determined by the ratio of the area of peak **f** ($-\text{CH}_3$ in PPO arms) to that of peak **a** ($-\text{CH}_3$ in PEHO cores), and the results are listed in Table 1. The ^{13}C NMR spectra of PEHO core, P2 and P4 samples, including the ascriptions of signal peaks, are shown in Figure 2 as examples. As R_{feed} increases, the intensity

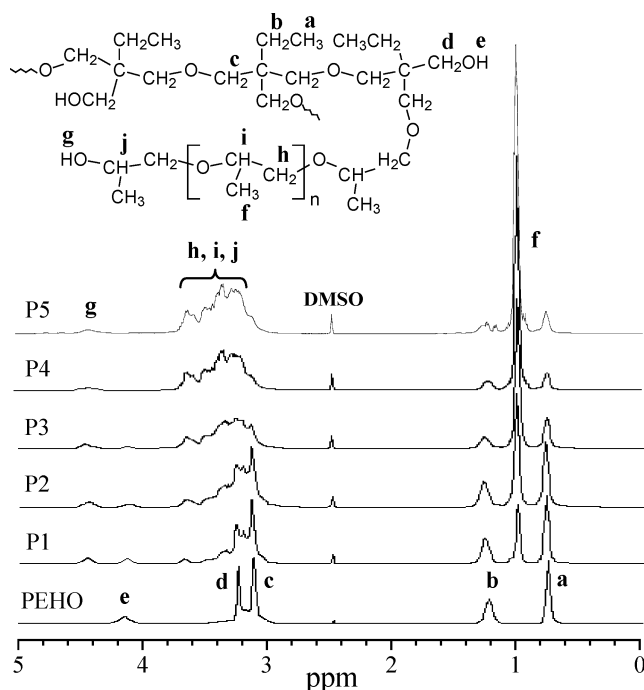


Figure 1. ^1H NMR spectra of PEHO core and PEHO-star-PPO samples.

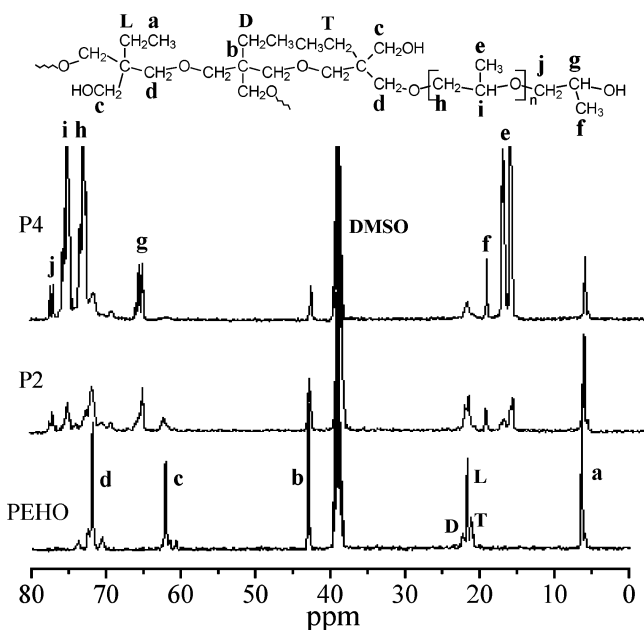


Figure 2. ^{13}C NMR spectra of PEHO core and PEHO-star-PPO samples P2 and P4.

of PPO peaks (**e**, **f**, **g**, **h**, **i**, and **j**)¹⁸ enhances whereas the intensity of PEHO peaks such as peak **c** and **T** decreases and almost disappears because PO has been covalently attached to PEHO cores. In the quantitative spectrum of PEHO, attention should be paid to the three peaks near 22.50 ppm, which belong to the carbon atoms of methylene in the ethyl groups of the dendritic unit (**D**), the linear unit (**L**), and the terminal unit (**T**). The degrees of branching (**DB**) of PEHO core precursors for PEHO-star-PPOs, being ~ 0.37 , can be determined by integration of the areas of the three peaks.¹⁹

To accurately determine the true M_n and PDI of hyperbranched polymers is an ever-present problem. Herein, we have tried to measure the relative M_n s of PEHO-star-PPOs by both SEC and NMR. The results

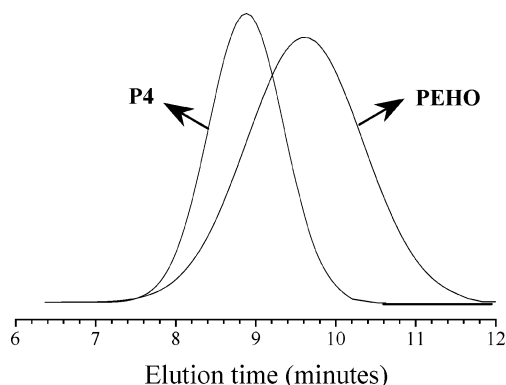


Figure 3. SEC curves of sample P4.

are listed in Table 1, and the SEC traces of P4 are shown in Figure 3 as an example. Obviously, $M_{n,SEC}$ of PEHO-*star*-PPO exhibits an increasing tendency as $R_{A/C}$ increases. Noteworthy, it is claimed that the observed $M_{n,SEC}$ may be lower than the actual M_n for hyperbranched polymers because the hydrodynamic volumes of hyperbranched polymers are smaller than those of linear polymers used for calibration, and hyperbranched polymers often exhibit adsorption by SEC columns due to their large number of end groups.²⁰ The data of $M_{n,NMR}$ well confirm the conclusion of SEC. Meanwhile, all PDIs of the copolyethers are relatively narrow (<1.72) and quite close to those reported by Frey et al. for the copolymers made from PPO and hyperbranched polyglycidol cores.¹⁸ Such narrow PDIs exclude the existence of considerable amounts of homopolymers. On the other hand, the PDI of hyperbranched star polymers with so many functional groups should be narrower according to the kinetic theory.²¹

The thermal behavior of PEHO-*star*-PPO samples was investigated with DSC and TGA. The curves of DSC and TGA are given in the Supporting Information (Figures S1 and S2), and the data of glass transition temperature (T_g) and decomposition temperature (T_d) are listed in Table 1. Both T_g and T_d of PEHO-*star*-PPO copolymers decrease with increasing $R_{A/C}$, which reflects the effect of PPO arms on the thermal properties of PEHO-*star*-PPOs.

Micellization of Ill-Defined PEHO-*star*-PPO Molecules. Unlike the molecules of PEHO-*star*-PEO, the molecules of PEHO-*star*-PPO are difficult to self-aggregate directly in water due to the smaller hydrophilicity of PPO. Therefore, the method of Eisenberg et al.

Table 2. Micelle Sizes Measured by TEM, SEM, and DLS

sample	$R_{A/C}$	D_{TEM} (nm)	D_{SEM} (nm)	$D_{h,DLS}$ (nm)
P1	0.8	252 ± 76	242 ± 82	294 ± 97
P2	1.6	219 ± 93	220 ± 100	255 ± 108
P3	4.0	167 ± 27	163 ± 20	201 ± 44
P4	6.8	134 ± 30	125 ± 45	159 ± 41
P5	9.2	121 ± 38	116 ± 41	140 ± 61

to create “crew-cut” aggregates was utilized.⁵ The hyperbranched copolymers were first dissolved in DMSO, a common solvent for PEHO cores and PPO arms. Then, the self-assembly of the copolymers was induced by addition of deionized water. The morphology of the aggregates was frozen by adding an excess of water. Finally, the solutions were dialyzed with a large amount of water to remove the residual DMSO before TEM, SEM, and DLS analyses.

Both TEM and SEM are the most powerful tools to directly observe the morphology and size of self-assembly objects. The photographs obtained by TEM are shown in Figure 4a–e, in which large regular spherical micelles can be clearly seen. The diameters (D_{TEM}) of the micelles measured statistically from the photographs are listed in Table 2. The average D_{TEM} of the micelles formed by different PEHO-*star*-PPO samples is larger than 100 nm and decreases in an orderly fashion as $R_{A/C}$ increases. SEM pictures are presented in the Supporting Information (Figure S3), and D_{SEM} of the micelles measured statistically from SEM photographs are also listed in Table 2. SEM results are well in agreement with TEM observations.

To better characterize the sizes of the obtained spherical micelles in solution, DLS was carried out to measure the hydrodynamic diameters (D_h) of the aggregates. The resultant DLS data are listed in Table 2, and the obtained plots of DLS are exhibited in Figure 5. The DLS data show that $\langle D_h \rangle$ (intensity-average D_h) decreases from ~ 300 to ~ 140 nm as $R_{A/C}$ increases from 0.8 to 9.2. Meanwhile, in every D_h distribution curve, only one peak can be observed. The peaks, especially those of samples P3–P5, are relatively narrow (PDIs are in the range of 0.01–0.04), which shows that the large micelles have a narrow size distribution.^{12a} We note that some smaller micelles observed in TEM and SEM are not found in DLS, and the average micelle size determined by DLS is larger than that measured by TEM or SEM (Table 2 and Figure 6). Müller et al.^{23a} also observed a similar phenomenon in their work. The difference is possibly induced in the process of preparing

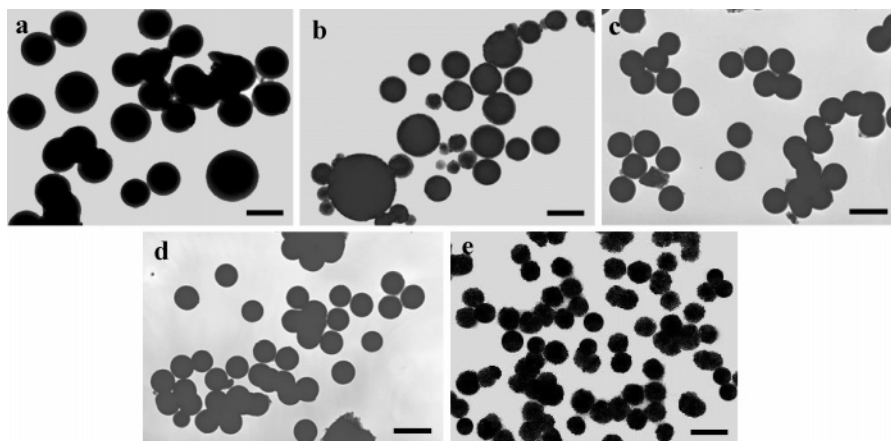


Figure 4. TEM photographs (a–e) of P1–P5: (a) P1 micelles, (b) P2 micelles, (c) P3 micelles, (d) P4 micelles, and (e) P5 micelles. The scale bars stand for 250 nm.

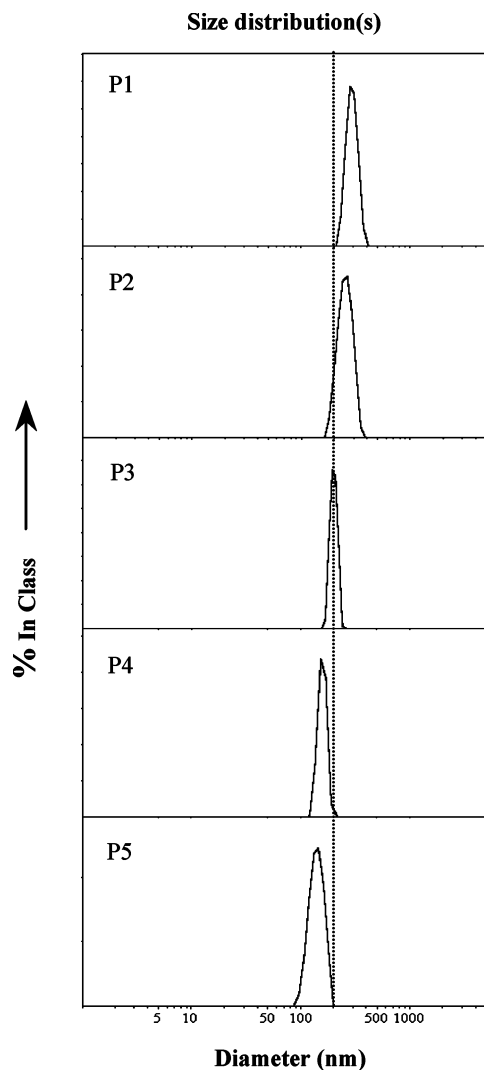


Figure 5. DLS plots of micelle solutions from PEHO-*star*-PPO samples.

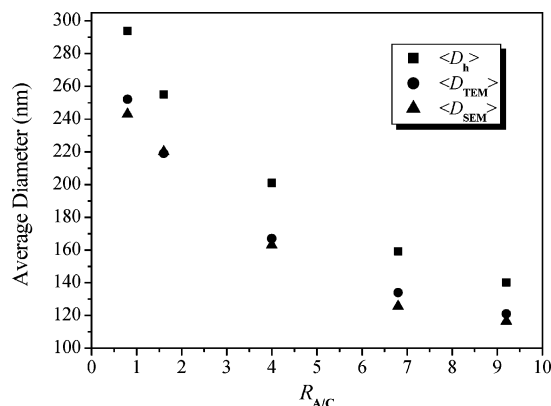


Figure 6. Dependence of average micelle diameters measured by DLS (■), TEM (●), and SEM (▲) on the R_{AC} of PEHO-*star*-PPO copolyethers.

samples of TEM or SEM. It is well-known that solvent evaporation may lead to the collapse, shrinkage, and even destruction of large micelles formed in solution, which result in the appearance of some smaller micelles and the reduction of the average micelle size; on the other hand, the slow solvent evaporation on the substrate can induce variations in concentration of micellar solution, which may also influence the micelle dimensions.²³

In summary, TEM, SEM, and DLS results clearly indicate that the ill-defined copolymer of PEHO-*star*-PPO can aggregate into large spherical micelles with controlled sizes dependent on the value of R_{AC} (Figure 6). In our previous work,^{10b} we have already found that the size of the vesicles (named as branched polymer-somes) formed by PEHO-*star*-PEO molecules decreased with increasing the hydrophilic volume fraction of the self-assembly precursors. Therefore, the dimensions of the aggregates resulting from both PEHO-*star*-PEO and PEHO-*star*-PPO copolyethers can be controlled by the molar ratio of hydrophilic arms to hydrophobic cores, i.e., the higher the value of R_{AC} , the smaller the size of the aggregates, which is identical with the conclusion of Eisenberg et al. for the aggregates originating from linear copolymers.^{5b}

On the other hand, according to the molecular weight and the structure of PEHO-*star*-PPO, the dimension of a single PEHO-*star*-PPO molecule should be less than 10 nm in the selective solvent of water. Therefore, PEHO-*star*-PPO molecules are too small to directly self-assemble into large micelles (over 100 nm) according to the conventional mechanism of self-assembly, which is valid for small micelles. Evidently, a more complex mode of aggregation must be developed for our self-assembly system. So, the aggregation mechanism of PEHO-*star*-PPO micelles should be studied.

The self-assembly mode of PEHO-*star*-PPO molecules is a big challenge for us to explore, which includes two aspects: one is the self-assembly interactions, and the other is the structure of the large micelles. We consider that the hydrophobic interaction, which is attributed to the amphiphilic characteristic of PEHO-*star*-PPO in water, and the intermicellar interactions such as hydrogen bonds (H-bonds) are responsible for driving the self-assembly. Herein, we tried to conduct some experiments to support the speculation.

First, the sample P2, as a representative, was end-capped by acetyl chloride according to the literature,^{10a} and the products with different efficiencies of end-capping (f) were obtained. The value of f can be determined by the ratio of the peak area of $-CH_3$ in acetyl group (~ 2.0 ppm) to that of $-CH_3$ in PEHO core (~ 0.8 ppm). The products with $f \approx 0.1$ (B) and 0.6 (C) were adopted to study their self-assembly behaviors at the same temperatures and concentrations. Obvious differences can be seen from the experiment phenomena (the photograph is shown in Figure S4 in the Supporting Information). The blue color of the micellar solution of B became weaker than that of micellar solution of P2 (A) without end-capping, and no blue color but some precipitate appeared for the solution of C. Correspondingly, $\langle D_h \rangle$ of the micelles of B measured by DLS sharply decreases to ~ 117 nm compared with that of the micelles of A (255 nm). For specimen C, $\langle D_h \rangle$ could not be detected by DLS, which means that product C is not able to self-assemble. Evidently, hydroxyl groups play an important role in the self-assembly of PEHO-*star*-PPO copolyethers. H-bonds will be formed between hydroxyl groups or between hydroxyl groups and ether oxygen atoms in the self-assembly process of PEHO-*star*-PPOs. So we think that the decrease in micelle size of B is a result of the decrease of hydroxyl groups that leads to the reduction of H-bonds. However, the deposition of sample C may be attributed to the further decreased hydrophilicity of PPO arms caused by too many end-capped acetyl groups, although the acetyl

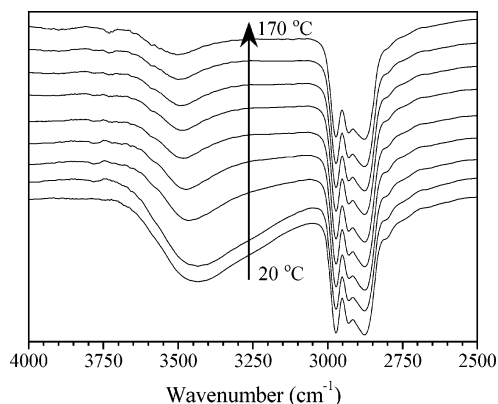


Figure 7. Variable temperature FTIR spectra of dried micelles formed by PEHO-*star*-PPO molecules (P2). The temperatures of the related curve from the bottom to the top are 20, 30, 50, 70, 90, 110, 130, 150, and 170 °C, respectively.

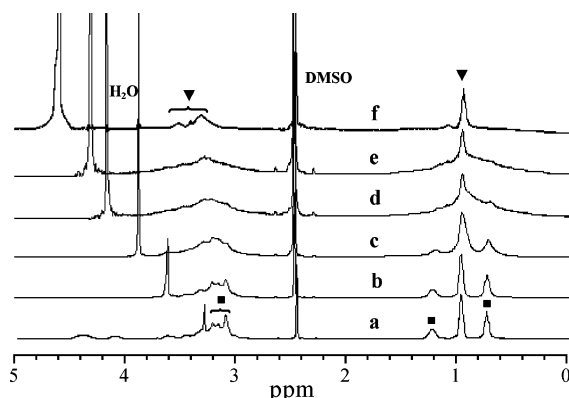


Figure 8. ^1H NMR spectra of PEHO-*star*-PPO molecules (P2) assembled in $\text{DMSO-}d_6$ and D_2O mixture. D_2O contents (vol %): (a) 0, (b) 9, (c) 16.7, (d) 28.6, (e) 50, and (f) 71.4. The symbol “■” expresses the peaks of PPO arms, and “▼” denotes the peaks of PEHO cores.

group is small. The effect of H-bonds on the self-assembly of PEHO-*star*-PPO will be further illustrated in Figure 9.

Second, variable temperature FTIR was used to detect H-bonds in the dried micelles. The spectra are provided in Figure 7. The peaks of methyl, methylene, or methenyl groups (from ~ 2875 to $\sim 2975\text{ cm}^{-1}$) were kept in the same position and intensity, which were used as inner standards. With increasing temperature from 20 to 170 °C, the peak of the hydroxyl groups (in the range $3000\text{--}3750\text{ cm}^{-1}$) gradually becomes narrower and shows blue shifts. This result indicates the existence of H-bonds in the micelles originating from PEHO-*star*-PPO molecules.^{10,24}

Finally, we used ^1H NMR to monitor the self-assembly process in order to obtain the information on molecular packing mode. Figure 8 presents the solution-state ^1H NMR spectra recorded continually at room temperature when various amount of D_2O was added into the $\text{DMSO-}d_6$ solution of PEHO-*star*-PPO. The peaks of $-\text{CH}_3$ in PPO ($\sim 1.0\text{ ppm}$) were kept in the same position and intensity as internal standards. With increasing D_2O , the self-assembly occurs while the peaks of PEHO gradually diminish and almost disappear, whereas the peaks of PPO still remain. The outcome demonstrates that PEHO cores are shielded by PPO arms in the resulting micelles.^{10b} In other words, PEHO cores are wrapped in the interior of the spherical micelle by PPO arms and the micelles hold a core-shell structure.³

Mortensen²⁵ has ever reported a structure of clusters, in which small micelles formed by PEO-PPO-PEO linear molecules were interconnected by the soluble PEO. Recently, we^{10a} have also found the macroscopic molecular self-assembly of PEHO-*star*-PPO molecules based on the interconnection of hydrophilic PEO lamellae. Taking account of the cluster structures and the aforementioned information, we suggest a possible self-assembly process for PEHO-*star*-PPO molecules and a new aggregate model coined by multimicelle aggregate (MMA) as shown in Figure 9. In the selective solvent of water, hyperbranched PEHO-*star*-PPO molecules spontaneously self-assemble into small micelles driven by hydrophobic interaction (Figure 9A,B). It is noticed that the smaller spherical objects observed in TEM and SEM images are probably the small micelles (Figure 4 and Figure S3). The small micelles presented here are similar to the conventional core-shell-type micelles with a small size less than 50 nm. In the small micelles, every PEHO-*star*-PPO molecule is speculated to separate into a squashed hydrophobic PEHO part and an extended hydrophilic PPO part. (The amphiphilic structure¹⁰ formed in microphase separation is shown in the magnified local section in Figure 9B.) The microphase-separated structure of hyperbranched PEHO-*star*-PPO molecules is similar to those suggested for other amphiphilic hyperbranched molecules,²⁶ amphiphilic dendrimers,^{8a-c} and amphiphilic starlike “Janus micelles”¹³ in selective solvents. The detailed studies on the microphase separation of PEHO-*star*-PPO molecules will be the topic of the next work of this laboratory.

The small micelle in Figure 9B is just an intermediate. Simultaneously, the small micelles, associated by intermicellar interactions such as H-bonds and van der Waals interactions, further aggregate into larger MMAs with a core-shell structure (Figure 9C). According to the MMA model, the data obtained from the end-capping experiment are not difficult to understand. The decrease of hydroxyl groups in end-capped PEHO-*star*-PPO molecules reduces the probability of forming H-bonds, therefore decreases the number of associated small micelles in a large micelle, and finally leads to the reduction of the dimensions of the large micelles.

Eisenberg and co-workers^{5a} pointed out that three sources are the major contributions to the thermodynamics of aggregation in micelles, namely, the core, the core-solvent interface, and the shell-solvent interaction. Among these, the former two sources make aggregates precipitate whereas the last one makes micelles dissolve. Considering the theory, the molecular structure of PEHO-*star*-PPO and Figure 9, we believe that the size decrease of the large micelles with increasing the R_{AC} of PEHO-*star*-PPO molecules is attributed to the interactions among the three sources. In addition, considering the intermediates of small micelles in MMA, intermicellar interactions such as H-bonds and van der Waals interactions should also be taken into account. Since all PEHO-*star*-PPO samples have an almost equirotal core, when R_{AC} is low, PEHO-*star*-PPO molecules have a small amount of hydrophilic PPO. Thus, more PEHO-*star*-PPO molecules are needed to aggregate together to balance the aforementioned interactions; otherwise, the sources that make molecules deposit would be larger than the shell-solvent interaction, leading to the precipitation of PEHO-*star*-PPO molecules. Moreover, the PEHO-*star*-PPO molecules with a smaller R_{AC} have a bigger density of hydroxyl

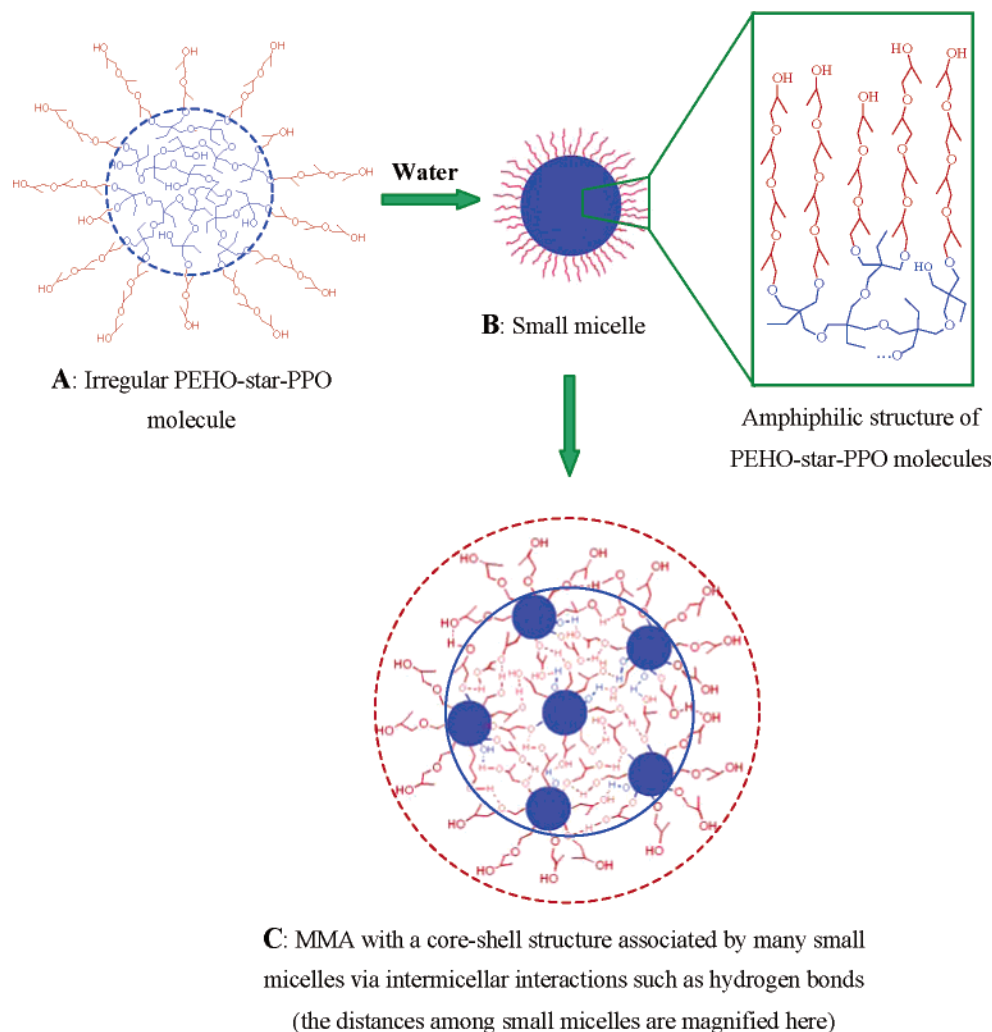


Figure 9. A possible self-assembly process of ill-defined PEHO-star-PPO molecules.

groups and a smaller steric hindrance,¹⁸ which is favorable for the association of small micelles by H-bonds according to MMA model, leading to the relatively big micelles. With increasing $R_{A/C}$, the amount of hydrophilic PPO increases. The enhanced interaction of shell-solvent and the decreased density of hydroxyl groups, as well as the increased steric hindrance, result in the aggregation of less PEHO-star-PPO molecules into large micelles according to MMA model. Consequently, the dimension of the obtained micelles decreases as $R_{A/C}$ rises.

On the other hand, all the obtained large micelles formed by different PEHO-star-PPO samples have a corresponding critical size, which should also be attributed to the balance of the interactions among the four sources mentioned above. For example, the intermicellar H-bonds interactions can facilitate the aggregation of small micelles into MMA, while the H-bond interactions between micelles and surrounding water molecules (so-called solvation) may prevent small micelles from further aggregating into MMA. Evidently, the equilibrium between the two interactions is one of the factors that decide the critical size of the large micelles. Müller and Abetz et al.^{23a} also found that the “supermicelles” aggregated by “Janus micelles” have a limited dimension.

This work proves that the ill-defined PEHO-star-PPO molecules can aggregate into well-defined spherical micelles, although the difference of hydrophilicity be-

tween the PPO arms and PEHO cores of PEHO-star-PPO molecules is small. Nevertheless, PEHO-star-PPO molecules cannot self-assemble into vesicles or macroscopic tubes like PEHO-star-PEO molecules. Perhaps, for the hyperbranched copolyethers, the morphology of the aggregates depends on the amphiphilic characteristics of the copolymers to some extent, which is deserved to be investigated continuously in the near future.

Conclusion

A series of hyperbranched multiarm copolyethers of PEHO-star-PPOs with different $R_{A/C}$ were synthesized. The results of NMR and SEC prove that PPO arms have been covalently attached to PEHO cores. Both T_g and T_d of PEHO-star-PPO copolymers decrease with increasing $R_{A/C}$. The self-assembly behavior of PEHO-star-PPO copolyethers was investigated by TEM, SEM, DLS, etc. The results indicate that the ill-defined PEHO-star-PPO molecules could aggregate into large regular spherical micelles with controlled size via the alteration of $R_{A/C}$. Then the self-assembly mechanism was explored by FT-IR, NMR, etc. In accordance with the molecular size of PEHO-star-PPOs and the big dimension of the resulting micelles, a possible self-assembly model named as MMA (Figure 9C) was suggested to clarify the formation of the large micelles.

Hopefully, PEHO-star-PPO micelles have a large number of hydroxyl groups on the outer surface, which

favor them potentials in some research fields such as organic functionalization, molecular nanocapsules, templates for preparation of mesoscale hollow spheres, and so on.

Acknowledgment. This work was sponsored by the National Natural Science Foundation of China (No. 20274024 and No. 50233030) and the Basic Research Foundation of Shanghai Science and Technique Committee (No. 03JC14046 and No. 04JC14057).

Supporting Information Available: DSC measurement (S1), TGA analysis (S2), SEM photographs (S3), and the various phenomena of the self-assembly of original and end-capped PEHO-*star*-PPO samples (S4). This material is available free of charge via the Internet at <http://pubs.acs.org>.

References and Notes

- (1) Bucknall, D. G.; Anderson, H. L. *Science* **2003**, *302*, 1904.
- (2) Antonietti, M.; Förster, S. *Adv. Mater.* **2003**, *15*, 1323.
- (3) Rösler, A.; Vandermeulen, G. W. M.; Klok, H. A. *Adv. Drug Deliver. Rev.* **2001**, *53*, 95.
- (4) Förster, S.; Antonietti, M. *Adv. Mater.* **1998**, *3*, 195.
- (5) (a) Zhang, L.; Eisenberg, A. *Science* **1995**, *268*, 1728. (b) Zhang, L.; Eisenberg, A. *J. Am. Chem. Soc.* **1996**, *118*, 3168. (c) Zhang, L.; Yu, K.; Eisenberg, A. *Science* **1996**, *272*, 1777. (d) Yu, K.; Eisenberg, A. *Macromolecules* **1996**, *29*, 6359. (e) Yu, Y.; Zhang, L.; Eisenberg, A. *Macromolecules* **1998**, *31*, 1144. (f) Zhang, L.; Eisenberg, A. *Polym. Adv. Technol.* **1998**, *9*, 677. (g) Discher, D. E.; Eisenberg, A. *Science* **2002**, *297*, 967.
- (6) (a) Discher, B. M.; Won, Y.-Y.; Ege, D.; Lee, J. C.-M.; Bates, F. S.; Discher, D. E.; Hammer, D. A. *Science* **1999**, *284*, 1143. (b) Bermudez, H.; Brannan, A. K.; Hammer, D. A.; Bates, F. S.; Discher, D. E. *Macromolecules* **2002**, *35*, 8203. (c) Hartgerink, J. D.; Beniash, E.; Stupp, S. I. *Science* **2001**, *294*, 1684. (d) Ludwigs, S.; Böker, A.; Voronov, A.; Rehse, N.; Magerle, R.; Krausch, G. *Nature (London)* **2003**, *2*, 744. (e) Loos, K.; Böker, A.; Zettl, H.; Zhang, M.; Krausch, G.; Müller, A. H. E. *Macromolecules* **2005**, *38*, 873.
- (7) (a) Ducharme, Y.; Wuest, J. D. *J. Org. Chem.* **1988**, *53*, 5787. (b) Menger, F. M. *Angew. Chem., Int. Ed. Engl.* **1995**, *34*, 2091. (c) Lee, M.; Cho, B.-K.; Kim, H.; Yoon, J.-Y.; Zin, W.-C. *J. Am. Chem. Soc.* **1998**, *120*, 9168. (d) Sijbesma, R. P.; Meijer, E. W. *Curr. Opin. Colloid Interface Sci.* **1999**, *4*, 24.
- (8) (a) Vanhest, J. C. M.; Delnoye, D. A. P.; Baars, M. W. P. L.; Vangenderen, M. H. P.; Meijer, E. W. *Science* **1995**, *268*, 1592. (b) Schenning, A. P. H. J.; Elissen-Roman, C.; Weener, J.-W.; Baars, M. W. P. L.; van der Gaast, S. J.; Meijer, E. W. *J. Am. Chem. Soc.* **1998**, *120*, 8199. (c) Wang, B.; Zhang, X.; Jia, X.; Li, Z.; Ji, Y.; Yang, L.; Wei, Y. *J. Am. Chem. Soc.* **2004**, *126*, 15180. (d) Freeman, A. W.; Vreekamp, R.; Fréchet, J. M. J. *Polym. Mater. Sci. Eng.* **1997**, *77*, 138. (e) Emrick, T.; Fréchet, J. M. J. *Curr. Opin. Colloid Interface Sci.* **1999**, *4*, 15. (f) Zeng, F.; Zimmerman, S. C. *Chem. Rev.* **1997**, *97*, 1681.
- (9) (a) Magnusson, H.; Malmström, E.; Hult, A. *Macromol. Rapid Commun.* **1999**, *20*, 453. (b) Bednarek, M.; Biedron, T.; Helinski, J.; Kaluzynski, K.; Kubisa, P.; Penczek, S. *Macromol. Rapid Commun.* **1999**, *20*, 369. (c) Yan, D.; Hou, J.; Zhu, X.; Kosman, J. J.; Wu, H. S. *Macromol. Rapid Commun.* **2000**, *21*, 557. (d) Mai, Y.; Zhou, Y.; Yan, D.; Lu, H. *Macromolecules* **2003**, *36*, 9667.
- (10) (a) Yan, D.; Zhou, Y.; Hou, J. *Science* **2004**, *303*, 65. (b) Zhou, Y.; Yan, D. *Angew. Chem., Int. Ed.* **2004**, *43*, 4896. (c) The hyperbranched poly[3-ethyl-3-(hydroxymethyl)oxetane] core in our previous paper was denoted as HBPO, and the multiarm copolymer with a HBPO core and PEO arms was denoted as HBPO-*star*-PEO. In this work, the same core is named as PEHO, and the copolymer is named as PEHO-*star*-PEO.
- (11) Xu, Y.; Gao, C.; Kong, H.; Yan, D.; Luo, P.; Li, W.; Mai, Y. *Macromolecules* **2004**, *37*, 6264.
- (12) For example: (a) Schilli, C. M.; Zhang, M.; Rizzardo, E.; Thang, S. H.; Chong, Y. K.; Edwards, K.; Karlsson, G.; Müller, A. H. E. *Macromolecules* **2004**, *37*, 7861. (b) Tu, Y.; Wang, X.; Zhang, H.; Fan, X.; Chen, X.; Zhou, Q.; Chau, K. *Macromolecules* **2003**, *36*, 6565. (c) Wang, C.; Ravi, P.; Tam, K. C.; Gan, L. H. *J. Phys. Chem. B* **2004**, *108*, 1621 and the works of Eisenberg et al. concerning small micelles, etc.
- (13) Erhardt, R.; Zhang, M.; Böker, A.; Zettl, H.; Abetz, C.; Frederik, P.; Krausch, G.; Abetz, V.; Müller, A. H. E. *J. Am. Chem. Soc.* **2003**, *125*, 3260.
- (14) Provencher, S. W. *Comput. Phys. Commun.* **1982**, *27*, 213.
- (15) Chu, B. *Laser Light Scattering: Basic Principles and Practice*, 2nd ed.; Academic Press: London, 1991.
- (16) (a) Sunder, A.; Quincy, M. F.; Mülhaupt, R.; Frey, H. *Angew. Chem., Int. Ed.* **1999**, *38*, 2928. (b) Sunder, A.; Krämer, M.; Hanselmann, R.; Mülhaupt, R.; Frey, H. *Angew. Chem., Int. Ed.* **1999**, *38*, 3552. (c) Sunder, A.; Mülhaupt, R.; Haag, R.; Frey, H. *Adv. Mater.* **2000**, *12*, 235. (d) He, X.; Yan, D.; Mai, Y. *Eur. Polym. J.* **2004**, *40*, 1759.
- (17) Roovers, J.; Zhou, L.; Toporowski, P. M.; Zwan, M.; Iatrou, H.; Hadjichristidis, N. *Macromolecules* **1993**, *26*, 4324.
- (18) (a) Sunder, A.; Mülhaupt, R.; Frey, H. *Macromolecules* **2000**, *33*, 309. (b) Knischka, R.; Lutz, P. J.; Sunder, A.; Mülhaupt, R.; Frey, H. *Macromolecules* **2000**, *33*, 315.
- (19) Hawker, C. J.; Lee, R.; Fréchet, J. M. J. *J. Am. Chem. Soc.* **1991**, *113*, 4583.
- (20) (a) Malmström, E.; Johansson, M.; Hult, A. *Macromolecules* **1995**, *28*, 1698. (b) Magnusson, H.; Malmström, E.; Hult, A.; Johansson, M. *Polymer* **2002**, *43*, 301. (c) Hawker, C. J.; Malmström, E.; Frank, C. W.; Kampf, J. P. *J. Am. Chem. Soc.* **1997**, *119*, 9903. (d) Uhrich, K. E.; Hawker, C. J.; Fréchet, J. M. J.; Turner, S. R. *Macromolecules* **1992**, *25*, 4583.
- (21) Yan, D.; Zhou, Z. *Macromolecules* **1999**, *32*, 819.
- (22) Mai, Y.; Zhou, Y.; Yan, D. *Chem. J. Chin. Univ.* **2004**, *25*, 1373.
- (23) (a) Erhardt, R.; Böker, A.; Zettl, H.; Kaya, H.; Pyckhout-Hintzen, W.; Krausch, G.; Abetz, V.; Müller, A. H. E. *Macromolecules* **2001**, *34*, 1069. (b) Yuan, X.; Jiang, M.; Zhao, H.; Wang, M.; Zhao, Y.; Wu, C. *Langmuir* **2001**, *17*, 6122. (c) Terreau, O.; Luo, L.; Eisenberg, A. *Langmuir* **2003**, *19*, 5601.
- (24) Gu, Y.; Kar, T.; Scheiner, S. *J. Am. Chem. Soc.* **1999**, *121*, 9411.
- (25) Mortensen, K. *Polym. Adv. Technol.* **2001**, *12*, 2.
- (26) (a) Ornatska, M.; Peleshanko, S.; Genson, K. L.; Rybak, B.; Bergman, K. N.; Tsukruk, V. V. *J. Am. Chem. Soc.* **2004**, *126*, 9675. (b) Zhai, X.; Peleshanko, S.; Klimenko, N. S.; Genson, K. L.; Vortman, M. Y.; Shevchenko, V. V.; Vaknin, D.; Tsukruk, V. V. *Macromolecules* **2003**, *36*, 3101.

MA051377Y